

REPRINT: differs from the original publication in layout but not in contents

This is the full-length reprint of the paper:

Chmielewski L. J. Detection of Non-parametric Lines by Evidence Accumulation...
Computational Imaging and Vision, Vol. 32, 2006. Springer-Verlag.

The original publication is available at <http://www.springerlink.com>

and as the following digital object: DOI:10.1007/1-4020-4179-9_54

The copyright owner of the paper is Springer-Verlag.

DETECTION OF NON-PARAMETRIC LINES BY EVIDENCE ACCUMULATION: FINDING BLOOD VESSELS IN MAMMOGRAMS*

Leszek J Chmielewski

Institute of Fundamental Technological Research, Polish Academy of Sciences
Świętokrzyska 21, PL 00-049 Warsaw, Poland

lchmiel@ippt.gov.pl

Abstract The evidence accumulation method for finding objects having shape which can be neither parameterized nor tabularized is proposed. The result is a multi-scale measure of existence of the detected object, in the accumulator congruent with the image domain, supplemented with local information on additional features of the object. The method is implemented for finding blood vessels in mammographic images, visible as bright lines. In this case, information from pairs of pixels is used for accumulation. The accumulation is fuzzy in several ways.

Keywords: Hough transform, evidence accumulation, fuzzy, non-parametric shapes, image domain, line detection, multi-scale, mammography, blood vessels detection

1. Introduction

The Hough transform (HT) ([1, 2], [3, 4], reviewed in [5], [6], [7]) and the related methods, called evidence accumulation [8] or evidence gathering [9], are the best choice for detection of objects in the presence of noise and occlusion. The necessary condition for using these methods is the possibility of representing the shape of the object of interest either in a parametric form (standard HT), or with the use of a template or table (generalized HT) [10, 11], or with the shape descriptors [9].

The method for finding objects having shapes which can be neither parameterized nor tabularized is proposed here. The algorithm uses heuristically chosen features of the detected shape. The accumulation is performed so that a multiscale measure of existence of the object sought, supplemented with the

*In: *Proc. Int. Conf. Computer Vision and Graphics ICCVG 2004*, pages 373-380, Warsaw, Poland, Sept 22-24, 2004. Vol. 32 in series: *Computational Imaging and Vision*, Springer.

local information on the important features of the object, emerges in the accumulator. The accumulator is congruent with the image domain. It can be analysed according to the needs posed by the application considered. Fuzzy accumulation is applied [12].

The method is implemented for the detection of bright lines (ridges), of various and slowly changing widths, with unpredictably changing direction. The feature of the bright line, chosen for the implementation, is that its edges have large gradients directed towards each other. Hence, pairs of pixels, lying each on the other side of the line, are considered in an elementary accumulation. The consistence of line direction is what makes the accumulation globally successful. The method can therefore be characterized as the multi-scale fuzzy evidence accumulation in the image domain, of the type m -to-1 [5], with $m=2$. The method is similar to the HT for circles [13, 14] in respect of accumulation in the image domain, and to the Symmetry Transform [15, 16] in respect of using pairs of pixels and consistence conditions. The differences are threefold: 1° the shape of the detected object is not parameterized; 2° the accumulation is multi-scale – it is performed simultaneously for a specified range of widths; 3° the value accumulated in a pixel for each width is complemented with the line direction information.

The motivation for the presented study was the detection of blood vessels in mammographic images. The final aim is the elimination of false classifications of the breast tumours as malignant, resulting from erroneous qualification of microcalcifications lying inside vessels, which are benign as a rule [17]. Fragments of the vessels themselves are also sometimes misclassified as microcalcifications. The feasibility study of such elimination is planned for the nearest future. The detection of blood vessels in mammograms with the standard HT was studied in [17] under the assumption of rectilinearity, which is removed here as untrue in general. In this paper we deal merely with the features of the algorithm itself. The vessels manifest themselves as bright lines having relatively fuzzy edges. The quality of the images (see Fig. 1 for an example) normally excludes the application of typical line detection algorithms [18, 19].

The proposed method has relatively high complexity, inherited both from the m -to-1 HT and from the Symmetry Transform. With the equipment currently available, images of moderate size can be analysed in acceptable time.

2. Algorithm

One of the images from The Mammographic Image Analysis Society database (MIAS) [20], which will be used to exemplify the considerations, is shown in Fig. 1 (image MDB005LL). Notations are shown in Fig. 2. Upper-case letters denote vectors. Pairs of pixels $p_i, i = 1, 2$ are considered in an elementary accumulation. Pixels in a pair are located at distances within a range

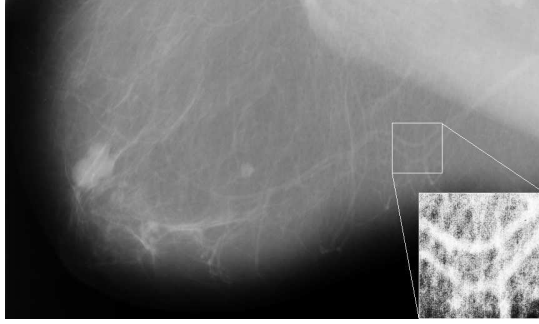


Figure 1. Example of a mammogram (4320×2600). A window shown with increased contrast.

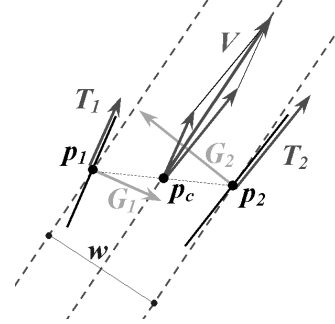


Figure 2. Construction of accumulated values (see text).

corresponding to the expected range of widths of the lines sought (actually, the analysed range is larger, to provide similar number of pairs irrespectively of line width; in this short paper this issue will be postponed). Each pixel is related to an edgel, shown as black line going through the pixel, having the *edgeness* (edge intensity) corresponding to the gradient G_i . The vectors T_i tangent to the edgels are the gradients rotated by $\pi/2$ in two opposite directions. The accumulation for each pair is performed in its central pixel p_c . Edgenesses, their consistence, and the consistence of their directions are used to form the accumulated value.

Necessary conditions. For each pixel p_1 , the second pixel p_2 is considered at the distances within the specified range. The gradient in each pixel must point towards the second pixel; for example, G_1 must form an acute angle with $\overline{p_1 p_2}$. The tangent vectors T_1, T_2 must form an acute angle. Image intensity values in all pixels of $\overline{p_1 p_2}$ must not be smaller than that in its darker end.

Direction, width and intensity. Line direction is the direction of the sum V of the tangent vectors T_i . The length $|V|$ is the basis for calculation of the line intensity to be accumulated. The line width w is the length of the projection of $\overline{p_1 p_2}$ onto the normal to V .

Penalty functions and \cos^2 function. Before accumulation, $|V|$ is multiplied by the penalty functions of directional consistence c_d and edgeness consistence c_e , defined as follows:

$$c_d = \cos^2[\angle(T_1, T_2)], \quad (1)$$

$$c_e = \cos^2[\pi (1 - \min(e_1, e_2) / \max(e_1, e_2)) / 2], \quad (2)$$

where e_i is the edgeness, $e_i = |G_i|$.

There is no penalty for acute angles formed by $\overline{p_1 p_2}$ and the line, so the evidence can be gathered from short as well as longer distances from p_c .

Note that the cosine square function, with a properly chosen frequency, has been used in both cases. This function has been used as the weighting function, or the membership function, throughout this paper. The shape of the function is similar to that of the Gaussian function, frequently used to model uncertainty, but has some valuable feature which will become apparent further.

Accumulated value and accumulator. The accumulated value – line intensity l – is calculated as

$$l = c_d c_e |V|. \quad (3)$$

The accumulator $L[x, y, w, \alpha]$ is four-dimensional, real-valued. The x, y are the image coordinates of the central pixel p_c of the pair and $x \in \langle 1, x_u \rangle$, $y \in \langle 1, y_u \rangle$; further, $w \in \langle w_l, w_u \rangle$ is the edge width, and α is its angle, $\alpha \in \langle 0, \pi \rangle$. Indexes l and u denote the lower (min) and upper (max) value, respectively.

Fuzzy accumulation. The algorithm is fuzzy in three respects. 1^o Actually, the accumulation is performed in a small 2×2 to 3×3 neighbourhood of the central pixel, which helps if this pixel should fall into non-integer coordinates. 2^o If during the accumulation, the intensity is fuzzified along the angle α with the membership function $\cos^2(\beta)$, $\beta \in \langle -\pi/2, \pi/2 \rangle$, which corresponds to $[\cos(2\beta) + 1]/2$, then instead of accumulation for α in a separate dimension of the accumulator, the known formula for adding the harmonics of the same frequency can be used, due to that the systematic additive and multiplicative constants are negligible in the accumulation. This leads to storing the current line intensity as amplitude and line direction as phase in a three-dimensional accumulator $L[x, y, w]$. 3^o After the accumulation is finished, the accumulator entries for each triplet (x, y, w) are fuzzified along the direction indicated by α . The range of fuzzification is chosen as $\pm 2w$, and as the membership function, the \cos^2 function, span along this range, is used one more time.

Results and postprocessing. The accumulator holds the line intensity and direction for each pixel of the image, at each line width within the specified range. The accumulated data should be analysed according to the requirements suitable for the given application. In the case of mammograms it is possible that bright lines representing various elongated objects like blood vessels, milk ducts and fibres of the breast tissue cross each other. In the presented method this phenomenon can be reflected in the accumulator array.

The condition of local homogeneity of line direction can be used to postprocess the results. In the present work this was calculated as the opposite of the standard deviation of angle in a circular neighbourhood of a pixel of radius w , mapped into an interval $\langle 0, 1 \rangle$ for the whole image.

A preliminary version of the analysis of the accumulated line intensity will be presented in the end of the next section.

Complexity and storage. To form a pair, for each pixel (x, y) a second pixel is taken from the ring with radii w_l, w_u (except its upper part, as that would lead to analysing each pair twice). The number of pairs is then proportional to $x_u y_u (w_u^2 - w_l^2)$ (in practice, not more than 20% of pairs meet the conditions). The fuzzification along the direction (point 3 in the paragraph on fuzzy accumulation above) is performed for $x_u y_u (w_u - w_l + 1)$ accumulator cells and spans along $(4w_u + 4w_l)/2$ pixels average for each cell, which leads to the same order as for the accumulation: $O(x_u y_u (w_u^2 - w_l^2))$. The storage requirements are of the order $O(x_u y_u (w_u - w_l))$. If the fuzzification were made during the accumulation, the complexity would increase with the factor of $2(w_u + w_l)$, and the storage would decrease by a component proportional to $x_u y_u$. Under the assumption that the image is square: $x_u = y_u = n$, and that the expected line widths are proportional to the image size n , we receive $O(n^4)$ for complexity and $O(n^3)$ for storage. As it will be shown in the next section, this does not exclude the effective execution of the algorithm, even with moderately equipped computers.

Parameters. It should be stressed that the only significant parameters of the algorithm are the limit edge widths w_l, w_u . The range of fuzzification in the image domain, fixed here to $\pm 2w$, and the size of the mask for the calculation of the gradient components, set to 5×5 , are the ‘hidden’ parameters which practically do not need tuning.

3. Example: issues of scale and complexity

Up till now, the algorithm was tested on around 20 images from the MIAS database. The relevance of results were consulted with the radiologists.

The algorithm is requiring so the question arises of the right scale at which the images should be analysed. To shed some light on this issue an example with three scales was performed. As an example, we shall present one result received for a window 400×400 of the image from Fig. 1 (upper left corner at pixel (3100, 1035)). The calculations were performed for three resolutions – full: 400×400 , edge widths $w \in \langle 24, 48 \rangle$, half: 200×200 , $w \in \langle 12, 24 \rangle$, and quarter: 100×100 , $w \in \langle 6, 12 \rangle$. Calculation times with a 1 GHz Pentium and memory requirements for a single-precision floating point accumulator were (55 min 25 s, 87 MB), (2 min 58 s, 13 MB), and (10 s, 2.7 MB), respectively. If the whole image of Fig. 1 were analysed at half scale, 2160×1300 , the requirements would be (228 min, 864 MB).

In the considered application it is not necessary to analyse the whole image, but only the regions suspected of carrying the disease. In general, however,

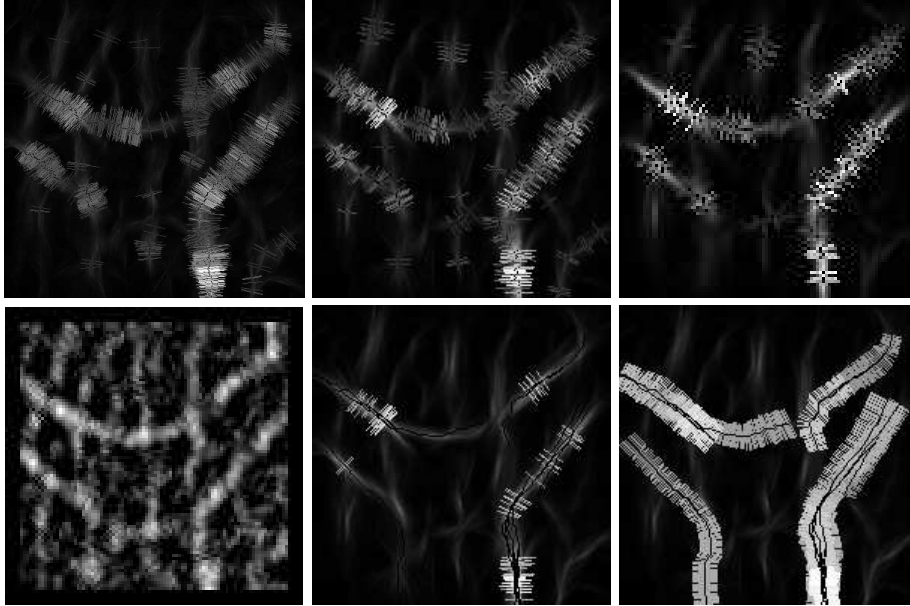


Figure 3. Results for window from Fig. 1. Upper left: full resolution 400×400 ; upper middle: half resolution 200×200 ; upper right: quarter resolution 100×100 ; lower left: result of Canny detector for quarter resolution; lower middle: possible central lines of vessels for half resolution; lower right: vessel widths overlaid. Transversal lines (brighter grey) representing vessel widths are normal to central lines (black), found starting from local maxima (black) – see text. Brighter lines are drawn over the darker ones.

also the algorithms which seem to pose elevated computational requirements should be explored. The development of the hardware, significant even at the low-cost end of the market, should not be overlooked.

The results for three resolutions are displayed in Fig. 3, together with the result of the Canny detector for the coarsest resolution, for comparison. The 3D result of accumulation has been projected onto the images in such a way that in each pixel the intensity found as the maximum for all widths is shown. Intensities are scaled to fit the image brightness range.

In the upper row of Fig. 3, local maxima of intensity for each width and short lines normal to the detected line of length equal to line width and brightness proportional to line intensity, are drawn. In the lower row, the results of a simple version of the line following algorithm are shown for the image in half scale (200×200), for which the results seemed the most realistic. The ridges of the accumulated value L were followed starting from the strong local maxima (larger than 0.5 of the strongest maximum). The next pixel was chosen as the one having the largest value from the six pixels found as follows. For the present width w in the accumulator array and its two neighbouring widths,

two pixels were considered, which determined the directions according to two roundings (up and down) of the local direction α . If any of these directions was in contradiction with the previous move, the respective pixel was rejected. The ridge following stopped if another ridge or image edge was reached, or if the accumulated value of the next pixel was too low (less than 0.25 of the average accumulated value for the currently analysed ridge).

The line following algorithm is in the preliminary stage of development. The thresholds used above are arbitrarily chosen. However, it seems that the expected actual lines are present among those starting from the maxima found. Therefore, the refinement of the method should lead to good results. Probably the way of fuzzifying the line intensity map can also be improved.

The presented example image contains fragments of two vessels (see Fig. 1). The shape of the upper vessel has been satisfactorily revealed by the algorithm, which is not the case for the lower vessel. This indicates that the local process of accumulation, although having relatively large range, can fail in finding the regional features of the image if they are locally ambiguous.

The results for three resolutions are qualitatively similar; however, the reduction of resolution makes some of the details disappear. Analysis in full resolution, generally typical for mammograms, seems not necessary as far as vessels are considered. An optimum resolution should be sought to reflect the scale of the detected objects.

Marginally it can be noted that even for the case of the coarsest scale the result of the proposed algorithm is more meaningful and bears more information than the result of such a typical line detector like the Canny detector.

4. Conclusion and further work

The information provided by the method is relatively rich and seems to reflect the human expectations concerning the locations of lines at regional scale. The presented method can not, however, reveal the large-scale continuity of lines, if this continuity is ambiguous at the regional scale.

The following issues need further work: 1^o reliable generation of continuous lines; 2^o optimal resolution and hierarchical analysis; 3^o differentiating line types by transversal brightness profile (hollow vessels, solid fibres), and finally 4^o testing the algorithm for its ability to reject the false positive qualification of mammograms due to the presence of microcalcifications in blood vessels.

Acknowledgments

The research described in this paper was supported by the (Polish) State Committee for Scientific Research grant No 7 T11E 037 21.

References

- [1] P. V. C. Hough. In *Proc. Int. Conf. on High Energy Accelerators and Instrumentation*. CERN, 1959.
- [2] P. V. C. Hough. A method and means for recognizing complex patterns. U. S. Patent 3.069.654, 1962.
- [3] A. Rosenfeld. *Picture Processing by Computer*. Academic Press, New York, 1969.
- [4] R. D. Duda and P. E. Hart. Use of the Hough transform to detect lines and curves in pictures. *Comm. Assoc. of Computing Machinery*, 15:11–15, 1972.
- [5] H. Maître. Un panorama de la transformation de Hough. *Traitement du Signal*, 2(4):305–317, 1985.
- [6] J. Illingworth and J. Kittler. A survey of the Hough transform. *Comp. Vision, Graph., and Image Proc.*, 44(1):87–116, 1988.
- [7] V. F. Leavers. Which Hough transform? *CVGIP-IU*, 58:250–264, 1993.
- [8] W. C. Y. Lam, M. T. S. Lam, K. S. Y. Yuen, and D. N. K. Leung. A general evidence accumulation technique for Hough transformation. In *Proc. IEEE Int. Conf. Systems, Man and Cybernetics*, volume 3, pages 2414–2419, Texas, USA, Oct 1994.
- [9] A.S. Aguado, M.S. Nixon, and E.M. Montiel. Parameterizing arbitrary shapes via Fourier descriptors for evidence-gathering extraction. *Comput. Vision and Image Underst.*, 69(2):202–211, Feb 1998.
- [10] P. M. Merlin and D. J. Farber. A parallel mechanism for detecting curves in pictures. *IEEE Trans. Comp.*, 24:96–98, 1975.
- [11] D. H. Ballard. Generalizing the Hough transform to detect arbitrary shapes. *PR*, 13:111–122, 1981.
- [12] O. Strauss. Use the Fuzzy Hough Transform towards reduction of the precision-uncertainty duality. *PR*, 32:1911–1922, 1999.
- [13] C. Kimme, D. Ballard, and J. Sklansky. Finding circles by an array of accumulators. *Comm. Assoc. of Computing Machinery*, 18(2):120–122, 1975.
- [14] W. C. Y. Lam and S. Y. Yuen. Efficient technique for circle detection using hypothesis filtering and Hough transform. *IEE Proc. - Vis. Image Signal Process.*, 143(5):292–300, Oct 1996.
- [15] D. Reissfeld, H. Wolfson, and Y. Yeshurun. Context-free attentional operators: the Generalised Symmetry Transform. *Int. J. Comput. Vision*, 14:119–130, 1995.
- [16] D. Reissfeld. The Constrained Phase Congruency Feature Detector: simultaneous localisation, classification and scale determination. *PRL*, 17(11):1161–1169, 1996.
- [17] F.L. Valverde, J. Munoz, R. Nishikawa, and K. Doi. Elimination of calcified false positives in detection of microcalcifications in mammograms using Hough transform. In *Proc. 5th Int. Workshop on Digital Mammography IWDM 2000*, pages 383–390, Toronto, Canada, Jun 11-14, 2000.
- [18] J. Canny. A computational approach to edge detection. *IEEE Trans. PAMI*, 8(6):679–698, 1986.
- [19] S. Castan, J. Zhao, and J. Shen. Optimal filter for edge detection. In *Proc. 1st European Conf. Computer Vision*, pages 13–17, Antibes, France, Apr 1990.
- [20] The Mammographic Image Analysis Society database.
<http://www.wiau.man.ac.uk/services/MIAS/MIASweb.html>, 2002.